STR on Interim Dry Storage of Commercial Spent Nuclear Fuel - An Update

Authors

Albert Machiels
Brentwood, California, USA

Peter Rudling
Tollered, Sweden

A.N.T. INTERNATIONAL®

Advanced Nuclear Technology International
Spinnerivägen 1, Mellersta Fabriken plan 4,
448 50 Tollered, Sweden

info@antinternational.com
www.antinternational.com

Ecolabelled printed matter, 4041 0799

Disclaimer

The information presented in this report has been compiled and analysed by Advanced Nuclear Technology International Europe AB (ANT International®) and its subcontractors. ANT International has exercised due diligence in this work, but does not warrant the accuracy or completeness of the information. ANT International does not assume any responsibility for any consequences as a result of the use of the information for any party, except a warranty for reasonable technical skill, which is limited to the amount paid for this report.

Quality-checked and authorized by:

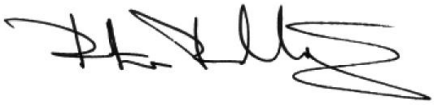

Mr Peter Rudling, Chairman of the Board of ANT International

Contents

1 Introduction

Except for a few countries (Finland, Sweden, France, and possibly Canada), the timing for establishing a geologic repository has been shown to be unpredictable. Therefore, spent fuel storage will remain the last backend operation for the foreseeable future in many countries. With proper attention, the radiological impact of storage is very low, but regulatory agencies have placed a heavy burden on licensees because of concerns related to the highly negative public perception related to the presence of spent fuel storage facilities in our biological environment. Therefore, locations where spent nuclear fuel (SNF) is or will be stored and their chosen storage technologies are the subjects of much scrutiny. Originally dry storage was intended to serve as a temporary solution for a few decades until final disposal; now, dry storage period is forecasted to be extended to 50, 60, or 100 years and even possibly longer. The focus of this review is on the spent nuclear fuel rods, and not on the storage system components such as the casks or the canisters and their internal hardware elements.

The intent of this STR is to provide information about some of the most important questions formulated by A.N.T. International clients.

After a short summary of Dry Storage Requirements in Section 2, the subsequent sections address the following customer questions:

- Update of “Back-end” issues in Section 3
- Thermal creep behaviour in relation to hydride reorientation in Section 4
- PWR fuel rod cladding failure due to the hydrogen migration in spent fuel in Section 5
- Update on any work on storage, transportation, long term issues in Section 6.
- Correlation between cooling rate and hydride reorientation in Section 7. In particular, the case of fast cooling when the cask containing SNF is flooded with water, from a cladding temperature of ~350°C to ~30°C, will be examined.

This report is an update of a previously issued ZIRAT25/IZNA20 STR on Interim Dry Storage of Commercial Spent Nuclear Fuel [Machiels A., 2021]and Dry Storage Handbook issued in 2017 [Patterson C. and Garzarolli F., 2015].

2 Overview of Regulations and Regulatory Guidance

This section is extracted from [Machiels A., 2021].

2.1 Basic Requirements [IAEA, 2012a]

Dry storage of spent LWR fuel has been safely implemented for over 40 years. The International Atomic Energy Agency (IAEA) Safety Standards Series No. SSG-15, Storage of Spent Nuclear Fuel, provides generic guidance for ensuring the safety of spent fuel storage. As stated in §1.3 of SSG-15:

> "The safety of a spent fuel storage facility, and the spent fuel stored within it, is ensured by: appropriate containment of the radionuclides involved, criticality safety, heat removal, radiation shielding and retrievability."

2.1.1 Containment

Containment prevents the release of radioactive material into the environment and is provided by the spent fuel cladding and the storage system (e.g., welded or bolted cask or welded canister). Therefore, maintaining spent fuel cladding integrity during dry storage is an important component of regulations.

For storage of spent fuel that has been characterized as failed or damaged, consideration of the condition of the fuel may lead to the inclusion of additional engineered methods for the safe handling of damaged fuel during loading and unloading, for examples, instrument tube tie rods for assemblies where stress corrosion cracking of the top nozzle is of concern, canning of damaged fuel assemblies to maintain spent configuration and ensure criticality control, and additional measures, such as encapsulation, to ensure the robustness of containment since, for damaged fuel, the primary containment feature, i.e., the spent fuel cladding, cannot be relied upon for control of the spent fuel material.

2.1.2 Criticality Safety

Criticality safety precludes an unplanned criticality event. Ensuring subcriticality often relies on geometry control. However, maintaining the geometry of spent fuel, especially during hypothetical accident conditions, may be challenging in terms of maintaining geometry. As a result, criticality control functions are often enhanced by other structures, systems and components (SSCs). These may include controlling fissile content, inclusion of neutron absorbers, and preclusion of moderators.

2.1.3 Decay Heat Removal

Effective removal of decay heat is important because degradation phenomena that could affect spent fuel integrity and some SSCs important to safety, such as polymers, are thermally activated.

2.1.4 Radiation Shielding

Shielding ensures that radiation exposure remains within safe limits and must be provided by the storage systems.

2.1.5 Retrievability

Retrievability is important to the extent that it may minimize the complexity, and thereby maximize the radiological safety, of subsequent spent fuel handling operations such as transportation and possible repackaging and conditioning before final storage in a geologic repository.

3 Status of the Alternative Fuel Performance Metrics PIRT Exercise

3.1 Introduction

Early results from the U.S. High Burnup Demonstration program, sponsored by the U.S. Department of Energy (DOE) and the Electric Power Research Institute (EPRI), showed that the thermal margins derived from measured vs. calculated temperature profiles inside a TN-32 cask, Figure 3-1, loaded with high burnup fuel were excessively large [EPRI Report, 2020a]. These results have provided a strong motivation for examining the U.S. nuclear industry's 30 years of experience with loading and maintenance of dry cask spent nuclear fuel (SNF) used for storage and transportation, with the purpose of identifying improvements in the regulatory framework for licensing these systems.

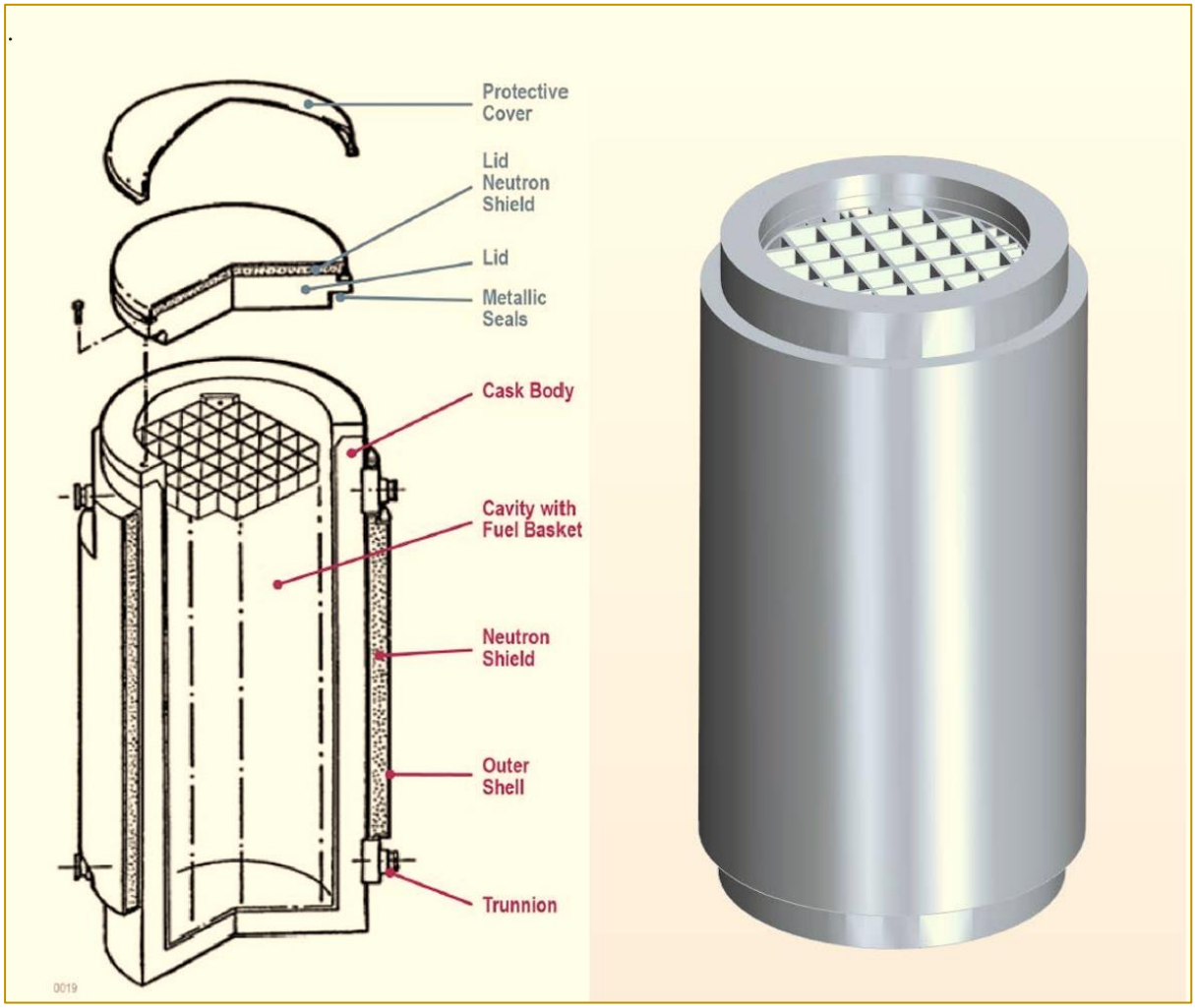

Figure 3-1: Diagram and geometry model for TN-32B dry storage cask, adapted from [Fort J.A. et al., 2019].

Sixteen recommendations, not requiring rulemaking, were developed and documented in an NEI White Paper [NEI Report, 2019]. According to the NEI White Paper, "meaningful improvements in regulatory efficiency should be achieved in a relatively short period of time and with minimal resources".

Section IV of the NEI White Paper is entitled "Guidance for Further Advancing the Definition of Performance Margin for Thermal Parameters". It contains five specific recommendations, including developing a thermal modeling metric, such as a peak cladding temperature limit (PCT), based on scientific information developed over the past 20 years. This section entitled "Alternate Fuel Performance Metrics"[1] refers to the ongoing re-examination of the current US guidance of using 400 °C as a "cliff edge" limit for the PCT. The objective is to identify candidate alternative fuel performance metrics that would be assessed for opportunities in providing additional operational flexibilities in the NRC guidance.

3.2 ZIRAT26 (Spring 2022) Presentation on "Thermal Margins Regulatory Issue Resolution"

Background, process, and progress as of March 2022 were presented during the Spring 2022 ZIRAT26 seminars [Machiels A., 2022]. A structured expert elicitation process, referred to as Phenomena Identification Ranking Table (PIRT), was used to examine spent fuel cladding performance (integrity) and gross cladding rupture.

The objective of the Spent Fuel Cladding Performance PIRT was to assess the significance and state of knowledge of parameters that may affect the integrity of spent nuclear fuel during dry storage and transport. Addressed phenomena consisted of creep (thermal and low temperature), diffusion-controlled cavity growth (DCCG), hydrogen embrittlement, delayed hydride cracking, hydride reorientation, thermal fatigue, mechanical fatigue, annealing, mechanical overload, fuel oxidation, and cladding oxidation. The results of the Spent Fuel Cladding Performance PIRT [EPRI Report, 2020b] listed several key takeaways and opportunities. For example, key takeaways included the absence of "cliff-edge" effects associated with a 400 °C PCT limit. They also identified knowledge gaps when considering PCT limits beyond the 400 °C. Opportunities included relaxation of the number of thermal cycles specified in the U.S. regulatory guidance as well as investigation of different temperature- and hoop-stress-stress-related criteria. During the PIRT exercise, the current definition of "gross rupture"[2] was recognized as being impractical during fuel selection practices. This created issues on how to discern whether the use of a damaged fuel can should be considered or not. Hence, it was recognized that an opportunity existed to enhance the analyses in determining when damaged fuel cans should be used in dry storage systems or transportation packages. A further discussion, with criticality, fuels/cladding and shielding experts, of the definition of "gross rupture", was recommended and subsequently addressed.

The objective of the Gross Rupture PIRT was to propose a better definition for the term "gross rupture" in the context of a safety objective focused on protecting fuel cladding integrity for spent fuel storage and transportation in terms of thermal performance, criticality safety and radiological performance. Evaluated phenomena were fission gas and backfill gas releases (thermal), fuel reconfiguration (thermal, criticality, and radiological), canister release (radiological) and fuel oxidation (radiological). The results [EPRI, 2021] indicated that all phenomena were of low significance, except possibly for radiological performance during unloading scenarios.

A revised definition of gross rupture was finalized.

"A cladding gross rupture corresponds to a fuel cladding failure resulting in fuel material release (fragments of various sizes) that would require precautions beyond those that are routinely used at sites to load intact or canned fuel, to prevent significant fuel material release during handling (loading and unloading)."

The revised definition was considered to be an important step in addressing the next PIRT on alternative fuel performance metrics.

[1] Sometimes simply referred to as "Fuel Metrics"

[2] "Gross rupture" is an important concept in the U.S. regulations. 10 CFR 72.122(h)(1) stipulates "…The spent fuel cladding must be protected during storage against degradation that leads to gross ruptures …"

4 Effect of Hydride Orientation on Thermal Creep Deformation Rates

The Japan Nuclear Energy Safety Organization (JNES) concluded that the orientation of the zirconium hydrides did not appear to have an impact on thermal creep rates of irradiated Recrystallized Annealed (RX)[3] Zircaloy-2 and Cold Worked Stress Relieved Annealed (CWSR) Zircaloy-4 in the domain of testing temperatures and hoop stresses of interest to dry storage applications [Ito K. et al., 2004a], [Ito K. et al., 2004b] and [IAEA TECDOC-1680, 2012].

When the cladding hydrogen concentration is below the hydrogen solubility limit (TSSD) at the testing temperature, hydrides are not present during creep deformation and therefore hydride orientation is irrelevant. Specimens with a hydrogen concentration greater than the solubility limit at the testing temperature would be required for observing any effects due to the orientation of the residual hydrides that would be present at the testing temperature.

To this report's authors knowledge, there has not been any reported investigation that tested similar types of cladding, containing hydrides either with (mostly) circumferential hydrides or significant amounts of radial hydrides, which would allow to definitely conclude that hydride reorientation is not a factor affecting thermal creep rates.

The JNES investigation performed creep testing on irradiated BWR and PWR fuel claddings with the characteristics shown in Table 4-1. Fuel rods were defueled and segmented in 80- to 100-mm length. Unirradiated cladding from the same lots as the irradiated claddings were also tested.

Table 4-1: Main characteristics of irradiated Zircaloy claddings, adapted after [Ito K. et al., 2004a] and [Ito K. et al., 2004b].

	Cladding Type	Effective length (mm)	Hydrogen cont. (ppm)	Rod average burnup (GWd/t)	Rod average neutron fluence ($n/m^2(E>1MeV)$)
BWR	8 x 8, Zr-lined, RX	100	30 ~ 140	47 ~ 50	$8.7\sim 9.6 \times 10^{25}$
PWR	17 x17, Low-Sn Zircaloy-4, SR	80	40 ~ 310	34 ~ 46	$6.1\sim 8.2 \times 10^{25}$
					© ANT International, 2024

The hydrogen content tended to be low from 30 to 140 wppm for irradiated BWR cladding and 40 to 310 wppm for irradiated PWR cladding.

Creep testing was performed in two different experimental set-ups illustrated in Figure 4-1. Testing set-ups were referred as "Segmented system" or "Piping system".

[3] During fabrication, zirconium alloys harden, that is, as the amount of cold deformation increases, the metal becomes stronger (harder) and less ductile. Dependent upon the required strength needed of the tubular product to meet safety criteria, various combinations of final heat treatment temperature and time are used which results in either a RX, CWSR or pRX (partial recrystallized) structure. Heat treatment at a temperature of 550-600 °C in Zircaloy results in a fully RX material. The resulting microstructure is an equiaxed structure of the Zr grains with precipitates uniformly distributed. To increase the mechanical strength of the material, the final anneal can be done at a lower temperature to relieve residual stresses without recrystallisation, CWSR. Also, a partial RX, pRX, can be obtained with a temperature in between of that of RX and SRA resulting in an inhomogeneous microstructure of equiaxed and distorted grains.

In the segmented system, defueled cladding tube specimens were filled to a predetermined pressure with argon gas and end plugs were welded to the two extremities. The specimens were placed inside an electric furnace. At regular intervals, the specimens were removed from the furnace; creep strain was measured at room temperature using a profilometer laser system; specimens were re-introduced into the furnace, brought back to the testing temperature until the next measurement. This approach involved cooling of the pressurized specimen to room temperature prior to creep strain measurement. As cooling proceeded, soluble hydrogen reprecipitated as hydrides under decreasing (driven by cooling) internal pressure. Potential formation of radial hydrides is expected when the cladding hoop stress is greater than the reorientation threshold stress.

In the piping system, a plug was welded at one end of the defueled specimen and the other end was connected to a pressurizing system that maintained a constant argon gas pressure during testing. It is unclear from the JNES paper how creep strains were measured. The graphic in Figure 4-1 seems to indicate measurement at temperature inside the furnace, but it cannot be ruled out that the specimens were depressurized and measured at room temperature outside the furnace. This is not important as long as the specimens were not cooled under internal pressure prior to measuring creep strain. The use of the piping system was limited to the measurements of a few Zircaloy-4 specimens.

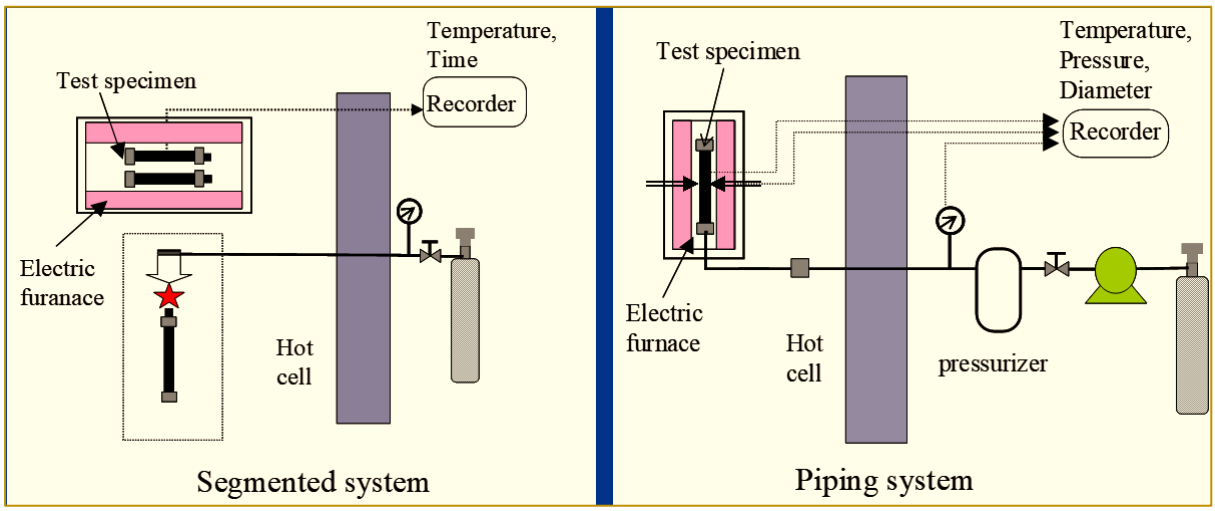

Figure 4-1: Creep test system referred to as either "segmented" (left) or "piping" (right), adapted after [Ito K. et al., 2004b].

Testing conditions were as follows:

- Temperatures: 330, 360, 390, and 420 °C. Corresponding hydrogen solubility limits cited by the investigators were respectively 90, 130, 180, and 230 wppm.
- Applied hoop stress ranged from 30 to 250 MPa for PWR Zircaloy-4 specimens and from 50 to 300 MPa for BWR Zircaloy-2 specimens.

As an example (test temperature = 360 °C), creep deformation data as a function of time for irradiated Zircaloy-4 and Zircaloy-2 are shown in Figure 4-2. To be noted is the very long testing duration (up to 8,000 h and 10,800 h for respectively Zircaloy-2 and Zircaloy-4).

5 PWR Fuel Rod Cladding Failure Due to the Hydrogen Migration in Spent Fuel Assembly

This topic is treated in Section 3.2.4 in [Machiels A., 2021]. Below is a short introduction and conclusion of this topic from [Machiels A., 2021].

Localized concentrations of hydrides that form by temperature-gradient-driven migration of soluble hydrogen along the length of SNF cladding is observed in-reactor and can adversely affect the integrity of an affected fuel rod; e.g., hydride lenses in fuel cladding at locations of spalled crud and oxide. Such a concentration process is also postulated to be a potential degradation mechanism in dry storage. The driving forces for axial migration and the formation of localized hydrides in fuel cladding are (1) concentration gradients that come from axial variations in corrosion and hydrogen pickup during operation, and (2) temperature gradients that exist in dry storage containers; temperatures of the end regions of fuel rods can be significantly lower than the peak temperature, Figure 5-1. The axial migration of hydrogen in SNF rods has been the topic of several investigations. Results to-date have ranged from no significant increase to some increase in hydrogen concentration at the ends of fuel rods. As a result, the issue of axial migration of hydrogen and localized degradation of cladding load-bearing capabilities has been cited as a potential performance issue during dry storage.

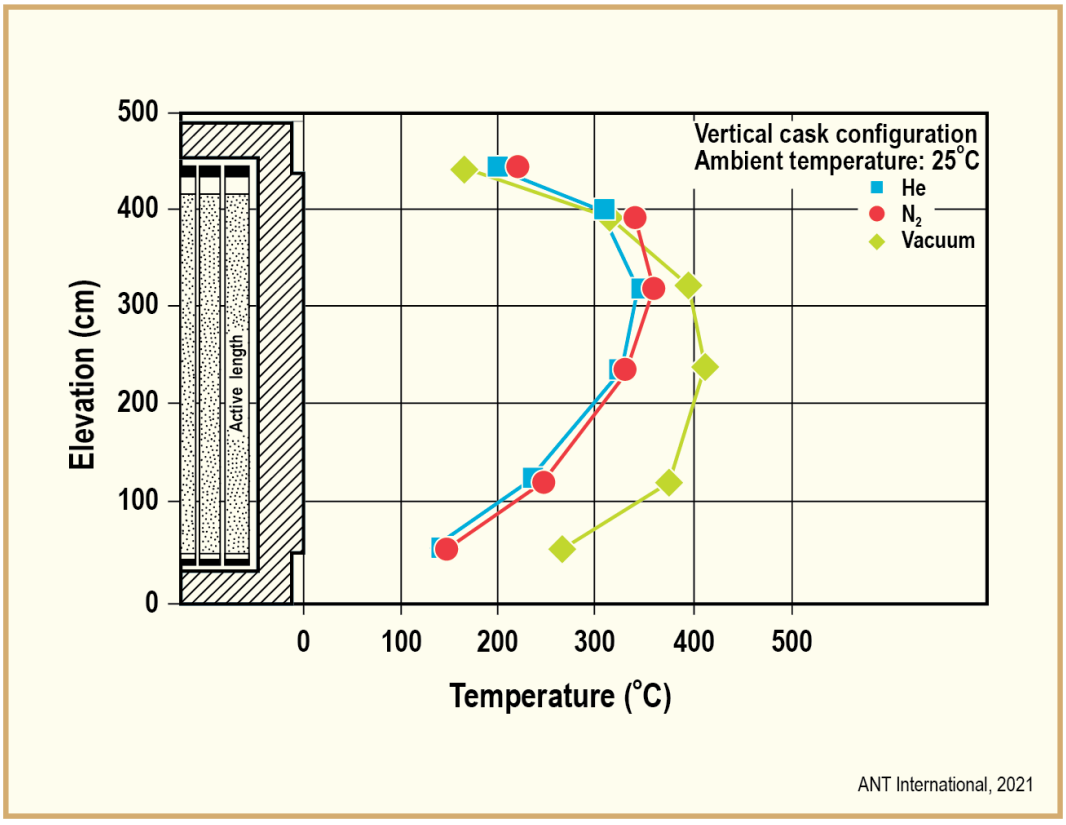

Figure 5-1: Axial temperature profiles in the CASTOR V/21 cask in the vertical position under vacuum or with He or N_2 backfill at about 1 atm [EPRI, 1986].

The migration of hydrogen along the length of a fuel rod (or guide tube) depends strongly on the temperature, temperature gradients and their variation with time. Although hydrogen is calculated to redistribute during early storage, the amount is small; i.e., no more than 10% to 20% of the initial concentration. In addition, with plausible decay histories, the falloff of temperature with dry storage time effectively freezes hydrogen in place; i.e., most axial migration occurs within the first few years. The likely time at high temperatures during the drying process (few hours) appears to be too short for appreciable axial redistribution. With the temperature variations expected in dry storage containers and the effects

6 Supporting Work on Storage, Transportation, Long-Term Issues

6.1 Introduction

As a part of the US Department of Energy (DOE) Office of Nuclear Energy (NE) High Burnup Spent Fuel Data Project, Oak Ridge National Laboratory (ORNL), Pacific Northwest National Laboratory (PNNL) and, Argonne National Laboratory (Argonne) are performing destructive examinations (DEs) of high burnup (HBU) (>45 GWd/MTU) spent nuclear fuel (SNF) rods from the North Anna Nuclear Power Station operated by Dominion Energy.

The goals of the High Burnup Spent Fuel Data Project are to "provide confirmatory data for model validation and potential improvement, provide input to future SNF dry storage cask design, support license renewals and new licenses for Independent Spent Fuel Storage Installations, and support transportation licensing for high burnup SNF" [EPRI, 2014].

Thirty-two high-burnup 17 x 17 PWR fuel assemblies from the North Anna Nuclear Power Station were loaded in a modified, instrumented TN-32B cask, Figure 3-1, or demo cask, and placed in dry storage in November 2017. Spent fuel assembly burnups ranged from 50 GWd/MTU to 55.5 GWd/MTU and included four different kinds of fuel rod cladding: standard Zircaloy-4 (Zirc-4), low-tin Zircaloy-4 (LT Zirc-4), ZIRconium Low Oxidation (ZIRLO), and M5 [S. Saltzstein et al., 2018] and [Montgomery R.A. et al., 2016]. Twenty-five rods, referred to as "sister" or "sibling" rods, having similar characteristics to the SNF fuel assembly rods were either extracted from the fuel assemblies that are actually stored in the demo cask or extracted from fuel assemblies of the same design and with the same characteristics as those stored in the demo cask. Details about the sister rods, their operation in the North Anna Nuclear Power Station, and the HBU Spent Fuel Data Project are provided in [EPRI, 2014], [S. Saltzstein et al., 2018], [Montgomery R.A. et al., 2016] and [Montgomery R.A. et al., 2019].

Examinations of the sibling rods are being performed to obtain a baseline of the HBU rod's condition before dry storage with a focus on understanding overall SNF rod strength and durability.

More specifically, the 25 sister rods were subjected to non-destructive examinations (NDEs) at ORNL's Irradiated Fuels Examination Laboratory (IFEL), as described in [Montgomery R.A. et al., 2019]. The NDEs included visual and dimensional inspections, gamma scanning, eddy current, and rod surface temperature measurements. Following the NDEs, 10 of the 25 sister rods were shipped from ORNL to Pacific Northwest National Laboratory (PNNL) for defueled cladding mechanical tests, see Figure 6-1. Several segments from the remaining 15 sister rods at ORNL were defueled and shipped to Argonne National Laboratory (Argonne).

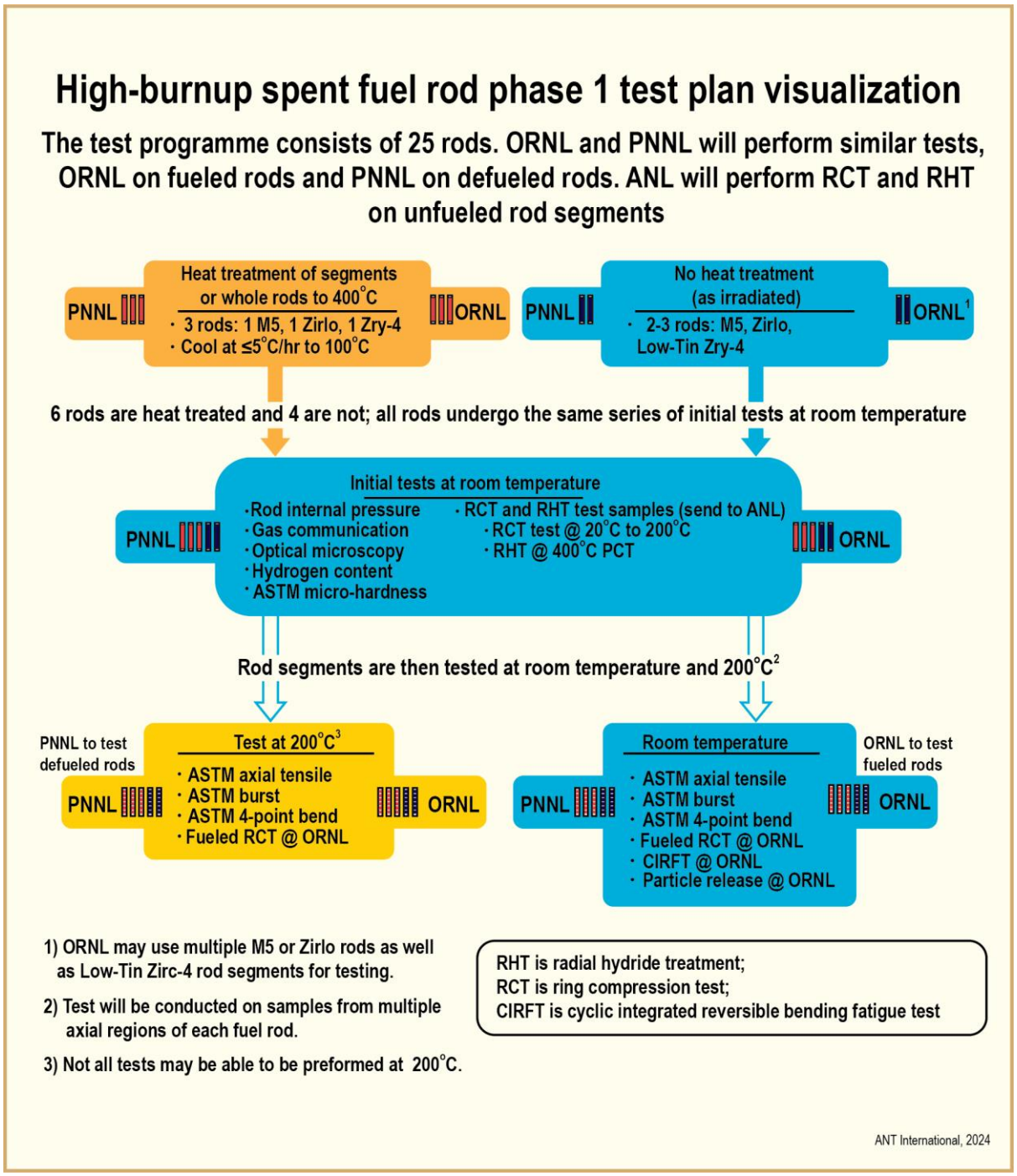

Figure 6-1: Phase 1 Test Plan Visualization [Saltzstein et al. 2018]. Note: RHT is radial hydride treatment, RCT is ring compression test, CIRFT is cyclic integrated reversible bending fatigue test [Shimskey RW et al., 2022a].

In the following sections the results are summarised from:

- ORNL [Montgomery R. and Bevard B., 2023] in Section 1.2,
- PNNL [Shimskey RW et al., 2022a] in Section 1.3 and,
- ANL [Billone M.C. et al., 2023] in Section 1.4.

7 Correlation Between Cooling Rate and Hydride Reorientation

7.1 Introduction

The thermal cycle for the spent nuclear fuel (SNF) transferred from a pool environment to a dry, inert environment is shown in Figure 7-1. The temperature is about 30 °C in the water storage pool at the reactor site. After loading the spent fuel assembly into the dry storage cask submerged in the storage pool, the water in the cask is removed and backfilled with helium (He) at a pressure of 0.1 MPa, or higher depending on the storage system design, Figure 7-2. The inferior cooling conditions after the water has been removed cause increases, over a relatively short time, of the fuel cladding temperature up to a maximum allowable temperature (specified or recommended by the country's regulatory authority), e.g., 400 °C in several countries. The reduction in decay heat over time will result in a progressive decrease in SNF cladding temperature.

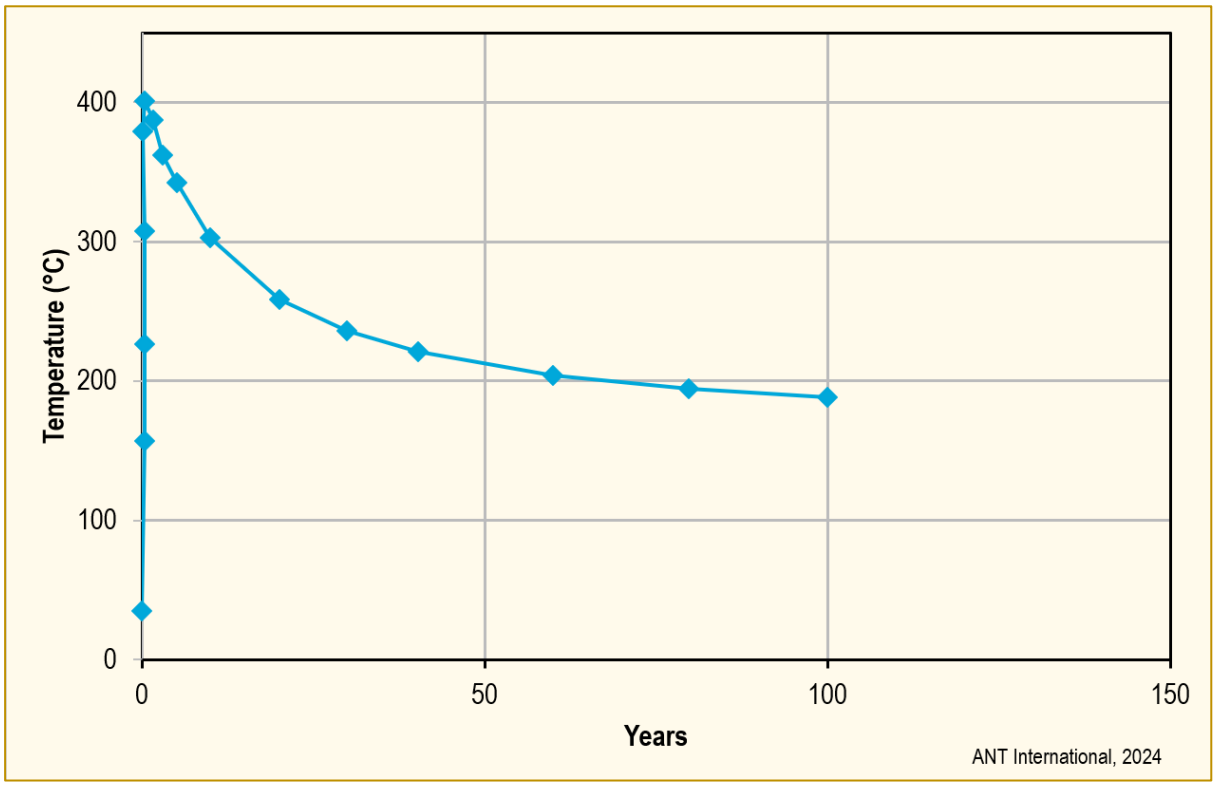

Figure 7-1: Temperature history in fuel claddings during interim dry storage.

Cooling rates during dry storage are typically < $3x10^{-3}$ °C/h, which cannot be readily reproduced in laboratory investigations due to time constraints. There is a need, however, to investigate the effect of cooling rate on zirconium hydride dissolution and re-precipitation that occur, respectively, during SNF heating and cooling, as shown in Figure 7-1. Hydrides, and particularly the orientation of the hydride platelets, can have a significant impact on cladding mechanical properties. Therefore, the sensitivity of hydride reorientation to cooling rate has been the subject of several notable investigations.

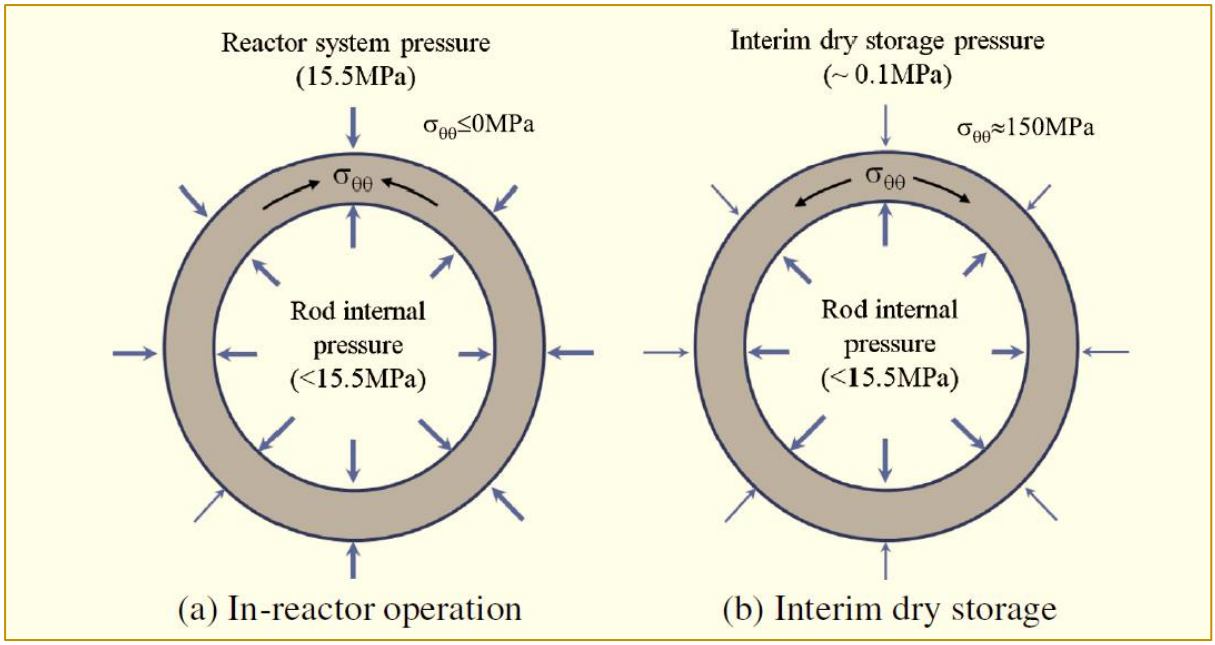

Figure 7-2: A schematic diagram of stress conditions of the cladding tubes, adapted from [Min et al., 2014].

7.2 Hydride Reorientation

Hydride reorientation (HRO) in spent fuel rod cladding is a mechanism that can occur as a result of a sequence of events that are inherent to dry storage operations. During reactor operation, part of the hydrogen formed by oxidation of the zirconium-based cladding by water is absorbed in the cladding alloy. Once the solubility limit of hydrogen in the cladding material matrix is reached, hydrogen precipitates in the form of zirconium hydride platelets mostly aligned along a circumferential direction, hence their name "circumferential hydrides", Figure 7-3(a). The mostly circumferential orientation of the hydrides in the discharged spent fuel rod claddings is a result of the cladding tube fabrication process and interplay between inner (inside the rod) and outer (reactor system) pressures during reactor operations; a reactor system pressure higher than the rod internal pressure, which is typical, results in compressive stress in the cladding. When the spent fuel is discharged from the reactor into the spent-fuel pool, tensile hoop stresses are created because the rod internal pressure is no longer compensated by the reactor system pressure, Figure 7-2. In addition, when the spent fuel is moved from wet to dry storage, fuel rod temperatures increase. The temperature increase results in dissolution of hydrides and in a corresponding increase of hydrogen in solid solution in the zirconium alloy matrix up to the temperature-dependent hydrogen solubility limit. Subsequent cooling during dry storage causes reprecipitation of the hydrides, possibly in a radial direction, Figure 7-3 (b), depending on the magnitude of the hoop stress that exists in the cladding.

8 References

Aomi M., Baba T., Miyashita T., Kamimura K., Yasuda T., Shinohara Y., Takeda T. *Evaluation of Hydride Reorientation Behaviour and Mechanical Properties for High-Burnup Fuel-Cladding Tubes in Interim Dry Storage*, Journal of ASTM International, Vol. 5, No. 9, JAI101262, 2008

Auzoux Q., Bouffioux P., Machiels A., Yagnik S., Bourdiliau B., Mallet C., Mozzani N., and Colas K., *Hydride reorientation and its impact on ambient temperature mechanical properties of high burn-up irradiated and unirradiated recrystallized Zircaloy-2 nuclear fuel cladding with an inner liner*, Journal of Nuclear Materials 494 pp. 114-126 (2017)

Billone M.C., *Ductility of High-Burnup-Fuel ZIRLO™ Following Drying and Storage*, ANL-19/14, M2SF-19AN010201011 Rev. 3, Argonne National Laboratory, June 2019.

Billone, M.C., T.A. Burtseva, Y. Chen and Z. Han, *Ductility of M5® and ZIRLO® Sibling Pin Cladding*, Argonne National Laboratory Report ANL-20/47, Nov. 17, 2020.

Billone M.C., Burtseva T.A., Chen Y., Han Z.," Ductility of Zircaloy-4 Sibling Pin Cladding", Spent Fuel and Waste Disposition", ANL Report M2SF-23AN010201012, ANL-22/69, 2023

Bouffioux P., Ambard A., Miquet A., Cappelare C., Auzoux Q., Bono M., Rabouille O., Allegre S., Chabretou V. and Scott C.P., *Hydride Reorientation in M5® Cladding and its Impact on Mechanical Properties*, Top Fuel 2013, Charlotte, North Carolina, USA, American Nuclear Society, 2013.

Cha H-J. et al., *Tensile hoop stress-, hydrogen content-, and cooling rate-dependent hydride reorientation behaviors of Zr alloy cladding tubes*, J. Nucl. Mater., 464, pp. 53-60, 2015

Colas, A. Motta, M.R. Daymond, J. Almer, Mechanisms of hydride reorientation in zircaloy-4 studied in situ, Zirconium Nucl. Ind. 17 (2014)

Cole, S.E. et al. *AREVA Optimized Fuel Rods for LWRs*. Proceedings of the Water Reactor Fuel Performance Meeting / Top Fuel 2012, (p. 230). Manchester, UK.

Courty O., Motta A.T. and Hales J.D., *Modeling and Simulation of Hydrogen Behavior in Zircaloy-4 Fuel Cladding*, J. Nucl. Mater., 452, pp. 311-320, 2014.

Courty O. F., Motta A. T., Piotrowski C. J. and Almer J. D., *Hydride precipitate kinetics in Zircaloy-4 studied using synchrotron X-ray diffraction*, J. Nucl. Mater., 461, pp.180-185, 2015.

EPRI, *The CASTOR-V/21 PWR Spent-Fuel Storage Cask: Testing and Analysis*, Electric Power Research Institute, Palo Alto, California, USA, 1986.

EPRI report 1009929 "*Spent Fuel Transportation Applications: Fuel Rod Failure Evaluation under Simulated Cask Side Drop Conditions*," EPRI, Palo Alto, CA: 1009929. 2005

EPRI, *End-of-Life Rod Internal Pressures in Spent Pressurized Water Reactor Fuel*, 3002001949, Palo Alto, California, 2013.

EPRI, *High Burnup Dry Storage Cask Research and Development Project: Final Test Plan*, contract no. DE-NE-0000593, Palo Alto, California, 2014.

EPRI (Electric Power Research Institute), *High Burnup Dry Storage Research Project Cask Loading and Initial Results*. Palo Alto, California. October 2019. 3002015076.

EPRI, *High-Burnup Used Fuel Dry Storage System Thermal Modeling Benchmark – Round Robin Results,* EPRI, Palo Alto, CA: 2020. 3002013124a

EPRI, *Phenomena Identification and Ranking Table (PIRT) Exercise for Used Fuel Cladding Performance*, EPRI, Palo Alto, CA: 2020. 3002018439b

EPRI, *Effect of Hydride Reorientation in Spent Fuel Cladding—Status from Twenty Years of Research*. EPRI, Palo Alto, CA: 2020c. 3002016033. https://www.epri.com/research/products/000000003002016033

EPRI, *Phenomena Identification and Ranking Table (PIRT) Exercise for Spent Fuel Cladding Gross Rupture*, EPRI, Palo Alto, CA: 2021. 3002020929

ESK, 2013. EMPFEHLUNG - Leitlinien für die Zwischenlagerung von radioaktiven Abfällen mit vernachlässigbaer Wärmeentwicklung (Revidierte Fassung vom 10.06.2013).

Fort J. A. et al.," *Thermal Modeling of the TN-32B Cask for the High Burnup Spent Fuel Data Project, Spent Fuel and Waste Disposition*", PNNL-28915, 2019.

Garde, Anand M., & Slagle, William H. (2009). *Hydrogen Pick Up Fraction for ZIRLOTM Cladding Corrosion and Resulting Impact on the Cladding Integrity*. Proceedings of the Water Reactor Fuel Performance Meeting – WRFPM / Top Fuel 2009, (p. 268). France.

IAEA, *Storage of Spent Nuclear Fuel* – Specific Safety Guide, IAEA Safety Standards Series No. SSG-15, International Atomic Energy Agency, Vienna (2012)a.

IAEA TECDOC-1680*, IAEA Spent Fuel Performance Assessment and Research: Final Report of a Coordinated Research Project (SPAR-II)*, page 56 (2012)

Ito K., Kamimura K., and Tsukuda Y., *Evaluation of Irradiation Effect on Spent Fuel Cladding Creep Properties*, Proceedings of the 2004 International Meeting on LWR Fuel Performance Orlando, Florida, September 19-22, 2004 Paper 1117a, (2004a).

Ito K., Kamimura K., and Tsukuda Y., *Evaluation of Irradiation Effect on Spent Fuel Cladding Creep Properties*, Proceedings of the 2004 International Meeting on LWR Fuel Performance Orlando, Florida, September 19-22, PowerPoint presentation (2004b).

JNES, 2010. Kamimura, K., Integrity Criteria of Spent Fuel for Dry Storage in Japan, International Seminar on Spent Fuel Storage (ISSF), Tokyo, Japan (2010).

Kalinina E.A. et. al., *Data Analysis of ENSA/DOE Rail Cask Tests*, SFWD-SFWST-2018-00049/ SAND2018-13258R (2018).

Kammenzind B. F., Franklin D. G., Peters H. R. and Duffin W. J., *Hydrogen pickup and redistribution in alpha-annealed Zircaloy-4*, Zirconium in the Nuclear Industry – 11th International Symposium, ASTM STP 1295, E. R. Bradley and G. P. Sabol, Eds., American Society for Testing and Materials, 338-370, West Conshohocken, PA, 1996.

Kaufholz P., et al., Journal of Nuclear Materials 510 (2018) 277- 281.

Kearns J., J. Nucl. Mater. 22 (1967) 292–303

Kim H., Kim I., Park S., Park J., Jeong Y., Korean J. Met. Mater. 48 (2010) 717.

Kitagawa et al. *Post Irradiation Examination of fuel rods in 55 GWd/t Lead Use Assembly*, Proc. of the 2005 Water Reactor Fuel Performance Conference, Kyoto, 2005.

Lacroix, E., A.T. Motta, and J.D. Almer, *Experimental Determination of Zirconium Hydride Precipitation and Dissolution in Zirconium Alloy*, Journal of Nuclear Materials 509 (2018) 162-167.

Lacroix, E., P.-C. Simon, A.T. Motta, and J.D. Almer, *Zirconium Hydride Precipitation and Dissolution Kinetics in Zirconium Alloys*, 19th International Symposium on Zirconium in the Nuclear Industry, May 20-23, 2019, Manchester, United Kingdom.

Machiels, A. 2005. "*Spent Fuel Transportation Applications: Fuel Rod Failure Evaluation under Simulated Cask Side Drop Conditions*," Electric Power Research Institute Report 1009929, Washington, DC.

Appendix A Hydride Reorientation

This information is extracted from Machiels A., "Interim Dry Storage", A.N.T. International Report, 2021.

A.1 Hydride Dissolution: Influence of Temperature

An important result established by [Kearns and Woods, 1966] was that reorientation of hydrides under external stress was associated only with precipitation during cooling and did not occur under isothermal conditions. Therefore, the maximum fraction of the hydride content that is susceptible to reorientation from circumferential to radial is limited by the temperature reached by the cladding. This temperature determines the extent of hydride dissolution, and correspondingly, how much hydrogen in solid solution could reprecipitate upon cooling. Table 7-1 provides concentrations of hydrogen in solid solution resulting from heating alpha-annealed Zircaloy-4 cladding containing a high enough hydride content [Kammenzind et al., 1996].

From Table 7-1, it can be deduced that no significant amount of re-orientation can be expected by limiting *peak* cladding temperatures < 250 °C, a temperature resulting, locally, in the creation of ≤ 40 wppm of hydrogen in solid solution and in low rod-average temperature and local cladding stresses. Again, it should be kept in mind that cladding temperatures are local and vary significantly in a cask. Peak cladding temperatures only affect a very small percentage of the cladding inventory, but typically serve as reference temperatures for assessing fuel rod performance.

A.2 Hydride Precipitation: Reorientation Threshold Stress

A minimum value of the cladding hoop stress is required before some indication of reorientation is first detected in cladding specimens subjected to a sequence of steps involving at least one heating followed by a cooling cycle during which tensile hoop stresses exist in the cladding.

An example of such a heat treatment in a laboratory setting would consist in (1) heating a cladding specimen from room temperature to a high temperature (≤ 400 °C); (2) pressurizing to achieve a pre-determined hoop stress in the cladding wall; (3) holding at the high temperature for a couple of hours, prior to (4) cooling at a pre-determined rate (average of 5 to 60 °C/hour), while maintaining a constant pressurization level or, alternatively, letting the stress decrease as the temperature does. By performing such thermo-mechanical treatments in research facilities, it is possible to mimic dry storage temperature/stress histories, except for the cooling rates, which, in actual dry storage systems, are several orders of magnitude lower (< 0.003 °C/hour) than in laboratory settings.

The reorientation threshold stress depends on many factors and should be regarded as very specific to the condition of the cladding material and heat-treatment parameters (temperature, hoop stress, and possibly cooling rate).

A.2.1 Effect of Temperature on Reorientation Threshold Stress

For cold-worked stress-relieved (CWSR) claddings, such as Standard Zircaloy-4 and ZIRLO™ with a hydrogen concentration > 200-300 wppm, Figure A-1 illustrates how the threshold hoop stress, in blue colour, varies as a function of cladding temperature and applied tensile stress during cooling to room temperature.

For combinations of temperature/hoop stress values on the left of the wide blue line, reorientation is not detected. For combination of temperature/hoop stress values on the right of the wide blue line, some reorientation is observed. The wide blue line, therefore, defines the value of the threshold hoop stress relative to the cladding temperature. The width of the blue line simply intends to convey that there is scatter in the reported data. As can be seen in Figure A-1, the threshold stress decreases with increasing temperature.

At any given temperature, the extent of reorientation becomes larger as the applied hoop stress increases beyond the threshold stress. The extent of reorientation as a function of applied hoop stress is usually represented by a sigmoid shape, as idealized in Figure A-2.

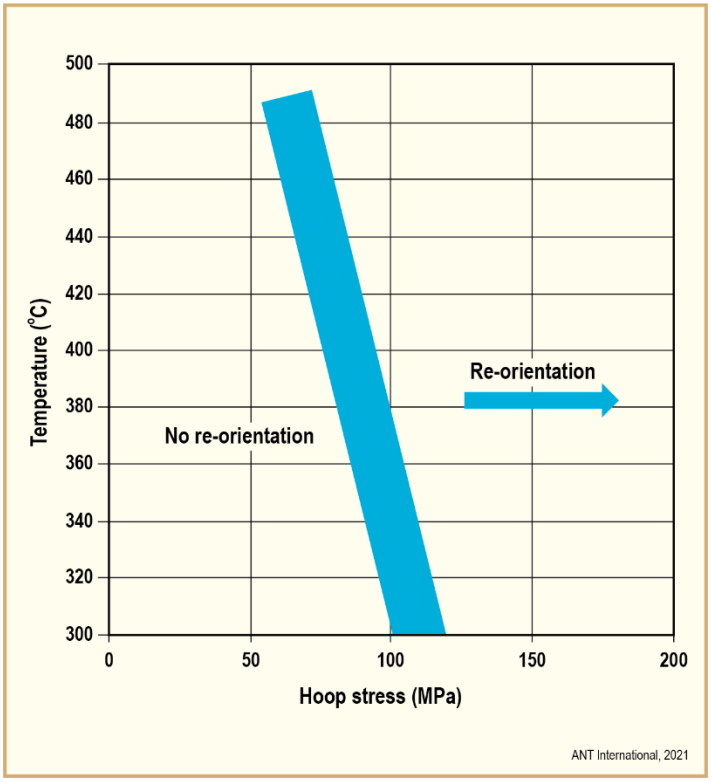

Figure A-1: Hydride reorientation mapping vs. temperature and applied stress. The thick, blue line indicates values of the reorientation threshold stress, i.e., minimum values of the applied hoop stress that are required before some reorientation is first reliably detected in cladding specimens (adapted from Section 7 in [EPRI, 2020a]).

Appendix B Theory of Hydride Stress Orienting Based on Classical Nucleation Models

This information is extracted from Puls M., "The Effect of Hydrogen and Hydrides on the Integrity of Zirconium Alloy Components, Hydride Reorientation", A.N.T. International Report, 2019.

B.1 Overall Theoretical Development

The foundations of the foregoing stress orienting models of Ells [Ells, 1970] and Puls [Puls, 1984a, 1986] are derived from classical nucleation models of liquid-gas and liquid-liquid systems of Vollmer and Weber [Vollmer & Weber, 1926]. By classical is meant that – starting from the embryonic state of the new phase – there is a finite difference in structure, state and/or composition between nucleus and parent phase with a sharp interface between the two. For a system held at constant temperature below the solvus temperature, formation of the new phase is thought to occur by random statistical fluctuations of clusters (embryos) of varying sizes in which the fluctuations have produced solute compositions close to those of the equilibrium coexistence compositions between bulk quantities of the two phases. Because of the presumed sharp interface between the two phases, surface energy is created. This surface energy makes an increasing contribution to the total Gibbs free energy change for formation of the embryo as it increases in size up to a maximum value above which further increases in size result in a diminishing contribution of the surface energy change to the change in total Gibbs free energy for precipitate formation. The critical size for formation of a stable nucleus for a given undercooling below the equilibrium (bulk property) solvus is the size at which the changes in surface energy result in a maximum in Gibbs free energy change.

The earliest applications of the foregoing models to solid-solid transformations of two-component, crystalline metallic solids were mostly to substitutional solid solutions. In such systems diffusion of the two components of the solid is by a vacancy mechanism and generally involves the diffusion of both solute and solvent species at temperatures when the transformation is kinetically feasible. In substitutional solid solutions the difference in atomic radii is generally small with the result that the stress-free misfit strains (i.e., the relative differences in sizes) between the unconstrained states of daughter and parent phases are also small. In addition, with solute/solvent diffusion governed by a vacancy mechanism, at temperatures where such diffusion is rapid the misfit strains between nucleus and matrix phases is often reduced by diffusion to negligible levels by vacancy accumulation along the interphase boundary, resulting in an incoherent interface between nucleus and matrix. This is not the case expected for the Zr-H system for which one can approximate the lattice Zr atoms as being immobile with only the interstitially located H atoms in the lattice being mobile. This assumption is the basis for the classical nucleation model described in the following.

The theory for hydride stress orienting given by Puls [Puls, 1984a, 1986] follows closely the methodology developed by Sauthoff for substitutional solid solutions [Sauthoff, 1975, 1976, 1977]. The purpose of the latter author's study was to determine which of the stages of nucleation, growth and coarsening played the dominant role in stress orienting of tetragonally misfitting Au-rich, plate-shaped precipitates in the Fe-Mo-Au alloy. Unlike the initial study of stress orienting for misfitting precipitates developed by Li for the nucleation stage subsequently adopted by Ells [Ells, 1970] for the nucleation and growth stages of hydride precipitates, Sauthoff's general relationships dealt with the effect of stress on all three stages of precipitate evolution: nucleation, growth and coarsening. Moreover, Sauthoff assumed that the precipitates formed would be coherent, or partially coherent, such that they would retain at least some of their tetragonal misfit strain with the matrix. The following is a brief outline of the Ells/Puls model for hydride orientation under stress in Zr and its alloys, updated to account for the solvus relationships derived in [Puls, 2012].

In classical nucleation theory the nucleation rate is given by

Equation B-1:

$$J^* = Z\beta^* \frac{N}{c_H^\beta} exp\left(-\frac{\Delta G^*}{k_B T}\right) exp\left(-\frac{\tau}{t}\right)$$

where J^* = time-dependent nucleation rate (the superscript $*$ denotes quantities evaluated at the size of the critical nucleus)

Z = Zeldovich non-equilibrium factor ($\approx 10^{-2}$ to 10^{-1})

β^* = rate at which atoms are added onto the critical nucleus

N = number of atomic nucleation sites per unit volume

c_H^β = atom (or mole) solute to solvent ratio (H/Zr in our case) in the critical nucleus (where β designates the precipitate phase, which for hydrides could be either the δ, γ or ε phase)

ΔG^* = free energy of activation for critical nucleus formation

τ = incubation time

t = isothermal reaction (hold) time

$k_B T$ = product of Boltzmann constant and absolute temperature, respectively

In Equation B-1, the Zeldovich factor accounts for the fact that some supercritical nuclei decompose and that *N* is an over estimate of the actual number of critical nuclei that can be formed at any one time.

It is assumed in Equation B-1 that the system has been abruptly brought to a state of super-saturation determined by the magnitude of the under-cooling from the equilibrium solvus which is the solvus corresponding to bulk quantities of the two phases at the isothermal hold temperature. This means that at the start of the isothermal hold time there would exist few, if any, metastable clusters of the precipitate phase. One would then expect there to be an incubation time, τ, before any critical nuclei would be formed after which there would be a short transient period of increasing nucleation rate followed by a regime during which there would be a constant (steady-state) increase in precipitate clusters. This steady state production of nuclei eventually would change to a decreasing, transient rate, terminating when the solute has been reduced to its equilibrium value.

The incubation time in Equation B-1 is approximated by Russell [Russell, 1971] as:

Equation B-2:

$$\tau = (2\beta^* Z^2)^{-1}$$

For hold times much greater than the incubation time, i.e., $t \gg \tau$, the bulk of the nuclei are formed at a constant, steady state rate, and it is over this regime that a meaningful comparison of the difference in nucleation rate for hydride platelets of different orientations with respect to an applied stress is obtained. That is, during steady state nucleation, the condition for the incubation time factor, $exp\left(-\frac{\tau}{t}\right) \rightarrow 1$, is assumed in Equation B-1. With this assumption, the steady state nucleation rate, J_{ss}^*, is given by:

Equation B-3:

$$J_{ss}^* = Z\beta^* \frac{N}{c_H^\beta} exp\left(-\frac{\Delta G^*}{k_B T}\right)$$

To determine the steady state nucleation rate, the factors Z and β^* need to be evaluated in addition to ΔG^*.

Appendix C References

Alam A.M. and Hellwig C., *Cladding Tube Deformation Test for Stress Reorientation of Hydrides,* J. ASTM Int. 5, Paper ID JAI101110, 2008

Aomi M., Baba T., Miyashita T., Kamimura K., Yasuda T., Shinohara Y., Takeda T. *Evaluation of Hydride Reorientation Behaviour and Mechanical Properties for High-Burnup Fuel-Cladding Tubes in Interim Dry Storage*, Journal of ASTM International, Vol. 5, No. 9, JAI101262, 2008

Aomi M., Baba T., Miyashita T., Kamimura K., Yasuda T., Shinohara Y., and Takeda T., *Evaluation of Hydride Reorientation Behaviour and Mechanical Properties for High-Burnup Fuel- Cladding Tubes in Interim Dry Storage*, Journal of ASTM International, Vol. 5, Issue 9, Paper ID JAI101262, 2009.

Auzoux Q., Bouffioux P., Machiels A., Yagnik S., Bourdiliau B., Mallet C., Mozzani N., and Colas K., *Hydride reorientation and its impact on ambient temperature mechanical properties of high burn-up irradiated and unirradiated recrystallized Zircaloy-2 nuclear fuel cladding with an inner liner*, Journal of Nuclear Materials 494 pp. 114-126 (2017)

Bai J.B., Ji N., Gilbon D., Prioul C., François D., Metall. Mater. Trans. A 25A (6) (1994).

Barberis P., Vauglin C., Fremiot P. and Guerin P., *Thermodynamics of Zr alloys: application to heterogeneous materials*, 17. ASTM International Symposium on Zirconium in the Nuclear Industry, Hyderabad, ASTM STP 1543, Feb. 2015.

Bouffioux P., Ambard A., Miquet A., Cappelare C., Auzoux Q., Bono M., Rabouille O., Allegre S., Chabretou V. and Scott C.P., *Hydride Reorientation in M5® Cladding and its Impact on Mechanical Properties*, Top Fuel 2013, Charlotte, North Carolina, USA, American Nuclear Society, 2013.

Carpenter G. J. C, *The dilatational misfit of zirconium hydride precipitated in Zr*, J. Nucl. Mater. 48, 1973.

Cha H-J. et al., *Tensile hoop stress-, hydrogen content-, and cooling rate-dependent hydride reorientation behaviors of Zr alloy cladding tubes*, J. Nucl. Mater., 464, pp. 53-60, 2015

Christian J.W., *The Theory of Transformations in Metals and Alloys*, Pergamon Press, Oxford, 1965

Chu H. C., Wu S. K., Chien K. F., Kuo R. C., *Effect of radial hydrides on the axial and hoop mechanical properties of Zircaloy-4 cladding*, Journal of Nuclear Materials, V. 362, pp. 93-103, 2007.

Chu H., Wu S. and Kuo R., *Hydride Reorientation in Zircaloy-4 Cladding*, Journal of Nuclear Materials, Vol. 373, 2008.

Daum R., Majumdar S., Liu Y. and Billone M., *Radial-hydride Embrittlement of High-burnup Zircaloy-4 Fuel Cladding*, Journal of Nuclear Science and Technology, Vol. 43, No.9, 2006.

Desquines, J., M. Puls, S. Charbaut, and M. Philippe, *Influence of Thermo-Mechanical Cycling on Pre-Hydrogenated Zircaloy-4 Embrittlement by Radial Hydrides*, Zirconium in the Nuclear Industry: 19th International Symposium, May 20-23, 2019, Manchester, United Kingdom.

Ells C. E., *Hydride Precipitates in Zirconium Alloys*, J. Nucl. Mater., Vol. 28, 1968.

Ells C., *The stress orientation of hydride in zirconium alloys*, Journal of Nuclear Materials, Vol. 35, pp. 306–315, 1970.

EPRI, *High-Burnup Used Fuel Dry Storage System Thermal Modeling Benchmark – Round Robin Results,* EPRI, Palo Alto, CA: 2020. 3002013124a

Fielding L.C.D., *The Bainite Controversy,* J. Mater. Sci. & Techno. 29, 2013.

Johnson W.C. et al., *Influence of Crystallography on Aspects of Solid-Solid Nucleation Theory*, Metall. Trans. A 6A, 1975.

Kammenzind B. F., Franklin D. G., Peters H. R. and Duffin W. J., *Hydrogen pickup and redistribution in alpha-annealed Zircaloy-4*, Zirconium in the Nuclear Industry – 11th International Symposium, ASTM STP 1295, E. R. Bradley and G. P. Sabol, Eds., American Society for Testing and Materials, 338-370, West Conshohocken, PA, 1996.

Kaufholz P., et al., Journal of Nuclear Materials 510 (2018) 277- 281.

Kearns J. and Woods C.R., *Effect of texture, grain size and cold work on the precipitation of oriented hydrides in Zircaloy tubing and plate*, Journal of Nuclear Materials, Vol. 20, 1966.

Kim, S.D., Y. Rhyim, J.S. Kim, and J. Yoon, *Characterization of Zirconium Hydrides in Zircaloy-4 Cladding with Respect to Cooling Rate*, Journal of Nuclear Materials, 465 (2015) 731-736.

Kono N. and Otsuka Y., *Dry Storage Fuel Long Term Integrity Confirmation Test – Irradiated BWR Fuel Cladding Creep Test: Creep Cladding Sample Failure*, Nuclear Power Engineering Corporation (NUPEC), March 12, 2003,

Lacroix, E., A.T. Motta, and J.D. Almer, *Experimental Determination of Zirconium Hydride Precipitation and Dissolution in Zirconium Alloy*, Journal of Nuclear Materials 509 (2018) 162-167.

Lacroix, E., P.-C. Simon, A.T. Motta, and J.D. Almer, *Zirconium Hydride Precipitation and Dissolution Kinetics in Zirconium Alloys*, 19th International Symposium on Zirconium in the Nuclear Industry, May 20-23, 2019, Manchester, United Kingdom.

Lee J.M., Kim H-A., Kook D-H., and Kim Y-S., *A study on the effects of hydrogen content and peak temperature on threshold stress for hydride reorientation in Zircaloy-4 cladding*, Journal of Nuclear Materials 509 (2018).

Machiels, A.J., *High Burnup – 10 Years Later*, Used Fuel and HLW Management Technical Advisory Committee, Washington, DC, September 13, 2012, ML12263A386.

Machiels, A.J., Y.R. Rashid, W.F. Lyon, and D.J. Sunderland, *Characterization of End-Of-Life Rod Internal Pressure in PWR Fuel*, Nuclear Engineering and Design. 324 (2017) 250–259.

Machiels A., "*STR on Interim Dry Storage of Commercial Spent Nuclear Fuel*", Advanced Nuclear Technology International (2021)

Mishima, Y., T. Okubo, and E. Sano, *Effect of Thermal Cycling on the Stress Orientation of Hydride in Zircaloy-2*, Metallurgical Transactions, *Vol. 2,* 1971, pp. 1995-1997.

Montgomery, R. and Bevard B., *Sister Rod Destructive Examinations (FY2020),* U.S. DOE, M2SF-1OR010201032 (2020).

Nagase F. and Fuketa T., *Influence of Hydride Re-orientation on BWR Cladding Rupture under Accident Conditions*, Journal of Nuclear Science and Technology, Vol. 41, No.12, p.1211-1217, December, 2004.

Papin J., Petit M., Grandjean C. and Georgenthum, V., *IRSN R&D Studies on High Burnup Fuel Behaviour under RIA and LOCA Conditions*, Top Fuel 2006, Salamanca, Spain, October, 2006.

Perovic V., Weatherly G.C. and Simpson C.J., *Hydride Precipitation in α/b Zirconium Alloys,* Acta Metall. 31, 1983.

Puls M.P., *Hydrogen-Induced Delayed Cracking: 2. Effect of Stress on Nucleation, Growth and Coarsening of Zirconium Hydride Precipitates,* Atomic Energy of Canada Limited Report, CRNL, Chalk River, Ontario, Canada, AECL-8381, 1984a.

Puls M.P., *Effect of Stress on Hydride Reorientation in Zirconium Alloys,* in: *Solute-Defect Interaction: Theory and Experiment*, Saimoto S., Purdy G.R., Kidson, G.V. (Eds.), Pergamon Press, 1986.

Puls M. P., *The Effect of Hydrogen and Hydrides on the Integrity of Zirconium Alloy Components, Engineering Materials*, DOI: 10.1007/978-1-4471-4195-2, Springer-Verlag, London, 2012.

List of Abbreviations

4PB	four-point bend
ANL	Argonne National Laboratory (USA)
ASTM	American Society for Testing and Materials
BWR	Boiling Water Reactor
CIRFT	Cyclic Integrated Reversible-Bending Fatigue Tester
CRUD	Chalk River Unidentified Deposits
CWSR	Cold Work and Stress Relieved
CWSRA	Cold-Work and Stress-Relief Annealed
DBTT	ductile-to-brittle transition temperature
DEs	destructive examinations
DHC	Delayed Hydride Cracking
DOE	US Department of Energy
DTT	ductility transition temperature
ENSA	Equipos Nucleares S.A.
ESK	Endlager-Kommission
FHT	full length heat-treated
GWd	gigawatt-days
HBU	high burnup
HCP	Hexagonal Close-Packed
HPUF	Hydrogen Pick-Up Fraction
HRO	Hydride reorientation
HRT	hydride redistribution tests
IAEA	International Atomic Energy Agency (Austria)
ID	Inner Diameter
IFEL	Irradiated Fuels Examination Laboratory
JNES	Japan Nuclear Energy Safety Organization
LWR	Light Water Reactor
LT	low-tin
M5	Cladding trademark of Framatome ANP (Zr-1.0Nb-0.13O by wt%)
MET	metallography
MMTA	multimodal transportation test
MPA	megapascal
MTU	metric tonne of uranium
NDE	non-destructive examinations
NE	Office of Nuclear Energy
NUPEC	Nuclear Power Engineering Corporation
NUREG	NRC Regulatory Guide
OD	Outer Diameter
ORNL	Oak Ridge National Laboratory
PCI	Pellet Cladding Interaction
PCT	Peak cladding temperature
PIE	post-irradiation examination
PIRT	Phenomena Identification Ranking Table
PNNL	Pacific Northwest National Laboratory
PWR	Pressurised Water Reactor
RCT	ring compression test
RHCF	radial hydride continuity factor
RHT	radial hydride treatment
RIP	rod internal pressure
RT	room temperature
RX	Recrystallised Annealed
R&D	Storage and Transportation Research and Development
SFWT	Spent Fuel & Waste Science and Technology
SNF	Spent Nuclear Fuel
SPH	spheroid
SRA	Stress Relieved Annealed
SSCs	structures, systems and components
TEPCO	Tokyo Electric Power Company Holdings, Inc.
TSSD	Temperature for Solubility during Dissolution
TSSP	Temperature for Solubility during Precipitation

Unit conversion

TEMPERATURE		
°C + 273.15 = K	°C × 1.8 + 32 = °F	
T(K)	T(°C)	T(°F)
273	**0**	32
289	16	61
298	25	77
373	**100**	212
473	**200**	392
573	**300**	572
633	360	680
673	**400**	752
773	**500**	932
783	510	950
793	520	968
823	550	1022
833	560	1040
873	**600**	1112
878	605	1121
893	620	1148
923	650	1202
973	**700**	1292
1023	750	1382
1053	780	1436
1073	**800**	1472
1136	863	1585
1143	870	1598
1173	**900**	1652
1273	**1000**	1832
1343	1070	1958
1478	1204	**2200**

Radioactivity	
1 Sv	= 100 Rem
1 Ci	= 3.7×10^{10} Bq = 37 GBq
1 Bq	= 1 s^{-1}

MASS	
kg	lbs
0.454	**1**
1	2.20

DISTANCE	
x (µm)	x (mils)
0.6	0.02
1	0.04
5	0.20
10	0.39
20	0.79
25	0.98
25.4	**1.00**
100	3.94

PRESSURE		
bar	MPa	psi
1	0.1	14
10	**1**	142
70	7	995
70.4	7.04	**1000**
100	10	1421
130	13	1847
155	15.5	2203
704	70.4	**10000**
1000	100	14211

STRESS INTENSITY FACTOR	
MPa√m	ksi√inch
0.91	**1**
1	1.10